Crystal-Plasticity Fundamentals

Henry R. Piehler, Carnegie Mellon University

THE PURPOSE of this article is to enable the reader to understand through examples the fundamentals of crystal plasticity. The rich historical development of crystal plasticity is traced in some detail to enable the reader to appreciate and critically analyze more sophisticated recent approaches to crystal-plasticity modeling. While most of the examples involve cubic metals deforming by rate-insensitive plastic flow, the concepts outlined here can be generalized to other crystal structures and loading conditions as well.

Schmid's Law

Crystal plasticity has as its origin Schmid's law, which states that crystallographic slip is initiated when a critical resolved shear stress on a slip plane in a slip direction is reached. As shown in Fig. 1, crystallographic slip initiates in uniaxial tension when the resolved shear stress on the slip plane in the slip direction reaches a critical value k (Ref 1). This critical resolved shear stress criterion can be expressed as:

$$\tau_{ns} = \sigma \cos\lambda \cos\phi = k \qquad \text{(Eq 1)}$$

where τ_{ns} is the shear stress on the slip plane, with normal n in the slip direction s; σ is the applied uniaxial stress; cos λ is the cosine of the angle between the tensile axis and the slip direction; cos φ is the cosine of the angle between the tensile axis and the slip plane normal; and k is the critical resolved shear stress. If $\hat{\mathbf{l}}$, $\hat{\mathbf{s}}$, and $\hat{\mathbf{n}}$ are unit vectors along the tensile axis l, the slip direction s, and the slip plane normal n, cos λ and cos ϕ can be found from the dot products $\hat{\mathbf{l}} \cdot \hat{\mathbf{s}}$ and $\hat{\mathbf{l}} \cdot \hat{\mathbf{n}}$.

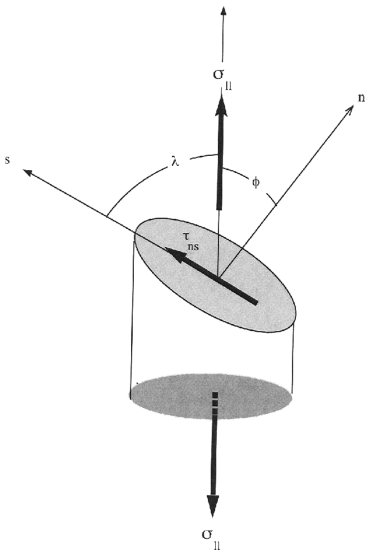

Fig. 1 Representation of Schmid's critical resolved shear stress criterion: $\tau_{ns} = \sigma \cos\lambda \cos\varphi = k$

For cubic metals, it is convenient to express the unit vectors $\hat{\mathbf{l}}$, $\hat{\mathbf{s}}$, and $\hat{\mathbf{n}}$ in terms of the unit vectors $\hat{\mathbf{i}}_1$, $\hat{\mathbf{i}}_2$, and $\hat{\mathbf{i}}_3$ along the [100], [010], and [001] crystallographic axes, respectively. For example, if a uniaxial stress is applied in the [001] direction of a face-centered cubic (fcc) single crystal, slip will occur on the (111) plane in the $[0\bar{1}1]$ direction when the normal stress σ reaches k/cos λ cos ϕ (Eq 1). For slip to occur on this $(111)[0\bar{1}1]$ slip system in response to a uniaxial normal stress applied along the [001] direction:

$$\hat{\mathbf{l}} = \hat{\mathbf{i}}_3, \hat{\mathbf{n}} = \frac{1}{\sqrt{3}}[\hat{\mathbf{i}}_1 + \hat{\mathbf{i}}_2 + \hat{\mathbf{i}}_3], \text{ and } \hat{\mathbf{s}} = \frac{1}{\sqrt{2}}[-\hat{\mathbf{i}}_2 + \hat{\mathbf{i}}_3]$$

Performing the dot products $\hat{\mathbf{l}} \cdot \hat{\mathbf{s}}$ and $\hat{\mathbf{l}} \cdot \hat{\mathbf{n}}$ yields:

$$\sigma_{[001]} = \sqrt{6}k = 2.45\,k$$

It should be noted that the yield stress must be at least 2 times the critical resolved shear stress, the minimum value achievable when both the slip plane normal and the slip direction are oriented at 45° to the uniaxial stress axis. As seen from Eq 1 and indicated in Table 1, Schmid's law is identical for fcc metals deforming on {111}<110> systems and body-centered cubic metals deforming on {110}<111> systems; only the identity of ϕ and λ are interchanged.

One of the earliest crystal-plasticity calculations was the determination by Sachs (Ref 2) of the uniaxial yield stress of an isotropic fcc metal in terms of the critical resolved shear stress k. Sachs' calculation was an average over the stereographic triangle of the uniaxial stresses necessary to initiate slip on the most highly stressed {111}<110> slip system(s). This isostress model predicted that the uniaxial yield stress of an isotropic fcc metal should equal 2.22k. It is also noteworthy that the single-crystal yield stress in the [111] direction is equal to:

$$1.5\sqrt{6}k$$

50% higher than the isostress yield stress for the [001] orientation calculated earlier and 65% above the Sachs average. It is this dependence of the single-crystal yield stress on crystallographic orientation that provides the basis for texture hardening (Ref 3).

Generalized Schmid's Law

Schmid's law for the response of crystals to a uniaxial normal stress can be generalized to three dimensions to include both normal and shear stresses. A critical resolved shear stress criterion can again be used, this time in response to all six components of stress, chosen initially for convenience along the cubic axes of an fcc crystal. These stresses along the cubic axes include the three normal stresses, σ_{11}, σ_{22}, σ_{33}, and the three independent shear stresses, $\sigma_{12} = \sigma_{21}$, $\sigma_{23} = \sigma_{32}$, and $\sigma_{31} = \sigma_{31}$. These stresses can be referred to as σ_{ij}, where i and j = 1, 2, 3.

Expressions for the resolved shear stresses on the twelve crystallographic slip systems (and their negatives) are written in terms of the six independent stresses referred to the cubic axes of the fcc crystal. The notation used by Bishop and Hill (Ref 4, 5) and Bishop (Ref 6) for the twelve slip systems is shown in Fig. 2 and Table 1, where the individual slip planes and their corresponding slip directions are identified, along with the shear strains associated with these systems. The generalized Schmid's law is obtained using a tensor transformation to sum the contributions to each of the twelve shear stresses from the stresses σ_{ij} along the cubic axes of the fcc crystal. This generalized Schmid's law for the critical resolved shear stress τ_{ns} on each of the twelve fcc slip systems is:

Table 1 Slip system notation used by Bishop and Hill for cubic crystals

Slip plane (or direction)	(111)	$(\bar{1}\bar{1}1)$	$(\bar{1}11)$	$(1\bar{1}1)$
Slip direction (or plane)	$[01\bar{1}][\bar{1}01][1\bar{1}0]$	$[0\bar{1}\bar{1}][101][\bar{1}10]$	$[01\bar{1}][101][\bar{1}\bar{1}0]$	$[0\bar{1}\bar{1}][\bar{1}01][110]$
Shear strain	a_1, a_2, a_3	b_1, b_2, b_3	c_1, c_2, c_3	d_1, d_2, d_3
Slip system designation	(a_1), (a_2), (a_3)	(b_1), (b_2), (b_3)	(c_1), (c_2), (c_3)	(d_1), (d_2), (d_3)

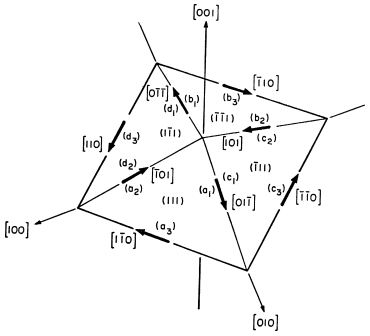

Fig. 2 Schematic representation of Bishop-Hill slip system notation

$$\tau_{ns} = l_{n1}l_{s1}\sigma_{11} + l_{n2}l_{s2}\sigma_{22} + l_{n3}l_{s3}\sigma_{33} + l_{n1}l_{s2}\sigma_{12} + l_{n2}l_{s3}\sigma_{23} + l_{n3}l_{s1}\sigma_{31} + l_{n2}l_{s1}\sigma_{21} + l_{n3}l_{s_2}\sigma_{32} + l_{n1}l_{s3}\sigma_{13} \quad \text{(Eq 2a)}$$

or

$$\tau_{ns} = \sum_{j=1}^{3}\sum_{i=1}^{3} l_{ni}l_{sj}\sigma_{ij} \quad \text{(Eq 2b)}$$

where l_{ni} and l_{sj} are the direction cosines of the angle between the particular slip plane normal n and the ith cubic axis and the direction cosine of the angle between the particular slip direction s and the jth cubic axis. Equation 2(a) can also be written using the summation convention that the repeated indices i and j are summed from 1 to 3, or:

$$\tau_{ns} = l_{ni}l_{sj}\sigma_{ij} \quad \text{(Eq 2c)}$$

These direction cosines can again be found from the dot products $l_{ni} = \hat{\mathbf{n}} \cdot \hat{\mathbf{i}}_i$ and $l_{sj} = \hat{\mathbf{s}} \cdot \hat{\mathbf{i}}_j$. Calculating the generalized Schmid's law for the $(111)[0\bar{1}1]$ system considered previously gives:

$$l_{n1} = l_{n2} = l_{n3} = \frac{1}{\sqrt{3}} \quad \text{and}$$
$$l_{s1} = 0, l_{s2} = -\frac{1}{\sqrt{2}}, l_{s3} = \frac{1}{\sqrt{2}}$$

and the generalized Schmid's law for this system becomes:

$$\tau_{ns} = \frac{1}{\sqrt{6}}(-\sigma_{22} + \sigma_{33} - \sigma_{12} + \sigma_{23} - \sigma_{32} + \sigma_{13})$$

Since $\sigma_{23} = \sigma_{32}$, this reduces to:

$$\tau_{ns} = \frac{1}{\sqrt{6}}(\sigma_{22} + \sigma_{33} - \sigma_{12} + \sigma_{13})$$

This $(111)[0\bar{1}1]$ system is designated as $-a_1$ by Bishop and Hill (Ref 4, Table 1), whose procedure will subsequently make use of all 12 of these generalized Schmid's law expressions. Notice that the critical resolved shear stress reduces to the same result calculated previously for uniaxial tension along the [001] direction if only σ_{33} is applied.

Taylor Model

G.I. Taylor (Ref 7) noted that the isostress model used by Sachs to calculate the uniaxial yield stress of an isotropic fcc aggregate in terms of the critical resolved shear stress k failed to satisfy the strain compatibility requirements among grains for plastic deformation of an isotropic material deformed in uniaxial tension. These isostrain uniaxial tension requirements are that, for a given plastic strain $d\varepsilon$ along the length l of a single crystal, the normal strains along two axes perpendicular to l are equal to $-d\varepsilon/2$ (from constancy of volume requirements), and all shear strains are equal to zero. Taylor then proceeded to calculate the uniaxial yield stress of an isotropic fcc aggregate in terms of the critical resolved shear stress using his isostrain model, which is described next.

Taylor's approach sought to determine the crystallographic shear strains resulting from the operation of a particular set of five independent slip systems that will accommodate the uniaxial tension isostrain requirements imposed along the primed axes associated with a particular fcc crystal orientation. The first step is to find the plastic strain increments referred to the cubic axes of an fcc single crystal resulting from the imposition of the plastic strains imposed along primed specimen axes. If the imposed strain increments along the primed specimen axes are designated as $d\varepsilon_{k'l'}$ using the summation convention, the strain increments along cubic axes can be written in terms of these imposed strains as:

$$d\varepsilon_{ij} = l_{ik'}l_{jl'}d\varepsilon_{k'l'} \quad \text{(Eq 3)}$$

The results of this isostrain requirement for uniaxial tension along various orientations can then be used to relate the plastic strains along the cubic axes and the contributions of each of the twelve possible slip systems (four <111> planes each containing three {110} slip directions), that is:

$$d\varepsilon_{ij} = \sum_{n=1}^{4}\sum_{s=1}^{3} l_{in}l_{js}d\varepsilon_{ns} \quad \text{(Eq 4a)}$$

where $d\varepsilon_{ns}$ is 1 of 12 true plastic strains associated with the operation of particular slip system with slip plane normal $\hat{\mathbf{n}}$ and a slip direction$\hat{\mathbf{s}}$. The true shear strain $d\varepsilon_{ns}$ is equal to ½ the simple shear strain γ_{ns}, which contains a rotation equal to (½) $d\gamma_{ns}$. This relationship between crystallographic or simple shear, pure or tensorial shear, and rotation is shown in Fig. 3. Using the nomenclature of Bishop and Hill contained in Table 1, the relationships between the five independent components of strain referred to the cubic axes and the12 crystallographic simple shear strains a_i (Eq 4a) become:

$$d\varepsilon_{11} = \frac{1}{\sqrt{6}}(-2a_2 + 2a_3 - 2a_5 + 2a_6 - 2a_8 + 2a_9 - 2a_{11} + 2a_{12})$$

$$d\varepsilon_{22} = \frac{1}{\sqrt{6}}(-2a_1 - 2a_3 + 2a_4 - 2a_6 + 2a_7 - 2a_9 + 2a_{10} - 2a_{12})$$

$$d\varepsilon_{33} = \frac{1}{\sqrt{6}}(+2a_1 + 2a_2 - 2a_4 - 2a_5 - 2a_7 - 2a_8 - 2a_{10} + 2a_{11})$$

$$d\varepsilon_{12} = \frac{1}{\sqrt{6}}(+a_1 - a_2 + a_4 - a_5 - a_7 + a_8 - a_{10} + a_{11})$$

$$d\varepsilon_{23} = \frac{1}{\sqrt{6}}(+a_2 - a_3 - a_5 + a_6 + a_8 - a_9 - a_{11} + a_{12})$$

$$d\varepsilon_{31} = \frac{1}{\sqrt{6}}(+a_1 + a_3 + a_4 - a_6 + a_7 - a_9 - a_{10} + a_{12}) \quad \text{(Eq 4b)}$$

Since there are five independent components of strain ε_{ij} along the cubic axes (reduced from six by the constancy of volume requirement $d\varepsilon_{11} + d\varepsilon_{22} + d\varepsilon_{33} = 0$), at least five slip systems (a's) must operate for Eq 4(b) to be inverted to find the amounts of shear on particular slip systems that must operate to accommodate the strains imposed along the cubic axes. This requirement for the simultaneous operation of five independent slip systems to accommodate an arbitrary strain state in an fcc crystal was first pointed out by von Mises (Ref 8). Since one can find more than one set of five independent shear strains to accommodate a given imposed strain state, the solution for ε_{ij} in terms of a_i (Eq 4b) is not unique.

Taylor selected the particular set of five independent crystallographic simple shear strains a_i that accommodated the imposed macroscopic strain state $\varepsilon_{k''l'}$ with a minimum of the total shear strain (or shear strain energy):

$$\sum_{i-1}^{5} a_i$$

Therefore, to calculate the value of the uniaxial yield stress for an isotropic fcc crystalline aggregate using Taylor's isostrain minimum

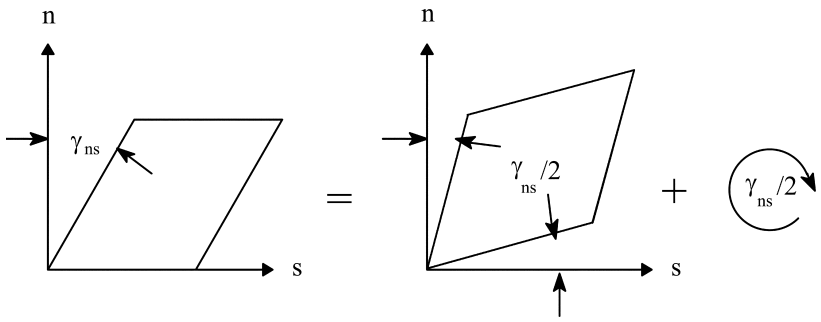

Fig. 3 Decomposition of a simple crystallographic shear into a pure or tensorial shear plus a rotation

shear criterion, one starts by imposing the plastic strain increment $d\varepsilon_{11} = d\varepsilon$ along the sample tensile axis and $-d\varepsilon/2$ along two axes perpendicular to this axis. This strain state referred to the sample axes is then transformed to the cubic axes of the fcc crystal using Eq 3. The particular set of five independent crystallographic shear strains a_i that accommodate the imposed strains is found next by looking for a set of five a_i's that satisfy Eq 4(b) and, at the same time, minimize the total crystallographic shear:

$$\sum_{i-1}^{5} a_i$$

Knowing the minimum total crystallographic shear for a particular crystal, one can find the value of the uniaxial yield stress in terms of the critical resolved shear stress k by equating the strain energy from slip to the external work done:

$$k\sum_{i-1}^{5} a_i = \sigma d\varepsilon$$

or

$$\sigma = k\sum_{i-1}^{5} a_i/d\varepsilon = Mk$$

where M, the ratio of the sum of the crystallographic shears to the uniaxial axisymmetric extension resulting from these shears, is the Taylor factor. More generally, M is defined as the sum of the crystallographic shears per unit effective strain.

Averaging the results for M over the stereographic triangle using this isostrain procedure, Taylor predicted that the uniaxial yield stress of an isotropic fcc aggregate is equal to 3.06k.

Taylor's minimum shear criterion was initially based on intuition but was later shown by Bishop and Hill (Ref 4, 5) to be rigorously correct and equivalent to their procedure described subsequently. Taylor also did not address the question as to whether or not one could find stress states that will simultaneously reach the critical resolved shear stress k on at least five independent slip systems while remaining below k on the remaining systems, a question that again was addressed subsequently by Bishop and Hill (Ref 4, 5). Even if such stress states could be found, however, the issue of stress compatibility across grain boundaries remained. Nevertheless, Taylor's isostrain model remains a significant advance in crystal plasticity and is also currently used as the basis for several numerical codes capable of calculating Taylor factors for arbitrary imposed strain states rather than just axisymmetric deformation.

Bishop-Hill Procedure

Like that of Taylor (Ref 7), the procedure of Bishop and Hill (Ref 4, 5) and Bishop (Ref 6) is an isostrain model. However, their stress-based approach sought to directly find stress states that could simultaneously operate at least five independent slip systems. Bishop and Hill began by examining the generalized Schmid's law requirements for operation of the 12 {111} <110> fcc slip systems. They chose to describe this yielding in terms of the new stresses:

$$A = \sigma_{22} - \sigma_{33}, B = \sigma_{33} - \sigma_{11}, C = \sigma_{11} - \sigma_{22}, F = \sigma_{23}, G = \sigma_{31}, \text{ and } H = \sigma_{12} \quad \text{(Eq 5)}$$

which leads to the 12 (24 with negatives) critical resolved shear stress expressions given in Table 2.

These 12 yield expressions (24 with negatives) can be plotted in three separate three-dimensional stress spaces having coordinates A, G, and H; B, H, and F; and C, F, and G. The yield condition for a particular slip system is represented by a plane in one of the three three-dimensional stress spaces. These planes make equal angles to the three coordinate axes; their intersection forms three separate octahedral, as shown in Fig. 4. The intersection of these planes along lines and at corners represents polyslip stress states. One notes that there are two types of polyslip stress states: one that is situated at the vertex of an octahedron (points x_1 and x_2 in Fig. 4) and the other that lies on a line oriented at 45° to two coordinate axes (points y_1, y_2, y_3, and y_4). The former will simultaneously operate four slip systems, the latter two. Hence, any polyslip stress state that simultaneously operates at least five slip systems will actually operate six or eight. Slip will be activated on eight slip systems if the stress state is located at two vertices (e.g., points x_1 and x_2) or at one vertex and two 45° lines (e.g., points x_1, y_1, y_2). Six systems will be activated if the stress state is located along three 45° lines (e.g., points y_1, y_3, and y_4). (One vertex and one 45° line would violate the condition that A + B + C = 0.) A summary of all permissible polyslip stress states is given in Table 2. The three cases considered previously correspond to stress states −2, −12, and −16. As can be shown with reference to the octahedral in Fig. 4, stress state −2 will operate the eight slip systems $-(a_2)$, (a_3), $-(b_2)$, (b_3), $-(c_2)$, (c_3), $-(d_2)$, and (d_3); stress state −12 will operate the eight systems $-(a_2)$, (a_3), $-(b_2)$, (b_3), $-(c_2)$, (c_3), $-(d_1)$, and (d_3); and stress state −16 will operate the six systems $-(b_2)$, (b_3), $-(c_1)$, (c_2), $-(d_1)$, and (d_3). A similar examination of the remaining polyslip stress states in Table 3 will show that the stress states 1 to 12 simultaneously operate eight slip systems, while stress states 13 to 28 operate six.

Table 2 Bishop-Hill shear stress expressions

Slip system	Yield expression
$\pm(a_1)$	$A - G + H = \pm\sqrt{6}\,k$
$\pm(a_2)$	$B - H + F = \pm\sqrt{6}\,k$
$\pm(a_3)$	$C - F + G = \pm\sqrt{6}\,k$
$\pm(b_1)$	$A + G + H = \pm\sqrt{6}\,k$
$\pm(b_2)$	$B - H - F = \pm\sqrt{6}\,k$
$\pm(b_3)$	$C + F - G = \pm\sqrt{6}\,k$
$\pm(c_1)$	$A + G - H = \pm\sqrt{6}\,k$
$\pm(c_2)$	$B + H + F = \pm\sqrt{6}\,k$
$\pm(c_3)$	$C - F - G = \pm\sqrt{6}\,k$
$\pm(d_1)$	$A - G - H = \pm\sqrt{6}\,k$
$\pm(d_2)$	$B + H - F = \pm\sqrt{6}\,k$
$\pm(d_3)$	$C + F + G = \pm\sqrt{6}\,k$

The particular state of stress that acts to accommodate an imposed state of strain can be found by selecting from the 28 (56 with negatives) permissible fcc polyslip stress states shown in Table 3, which shows the particular stress state that maximizes the external work done. This principle of maximum work was first derived rigorously by Bishop and Hill (Ref 4, 5), who also showed it to be equivalent to the minimum shear approach taken earlier by Taylor (Ref 7). The increment of work done, with reference to the cubic axes, is:

$$dW = \sigma_{11}d\varepsilon_{11} + \sigma_{22}d\varepsilon_{22} + \sigma_{33}d\varepsilon_{33} + 2\sigma_{12}d\varepsilon_{12} + 2\sigma_{23}d\varepsilon_{23} + 2\sigma_{31}d\varepsilon_{31} \quad \text{(Eq 6a)}$$

or, in Bishop-Hill notation:

$$dW = -Bd\varepsilon_{11} + Ad\varepsilon_{22} + 2Fd\varepsilon_{23} + 2Gd\varepsilon_{31} + 2Hd\varepsilon_{12} \quad \text{(Eq 6b)}$$

In the actual calculation procedure, the strain increments $d\varepsilon_{ij}$ along the cubic axes are first

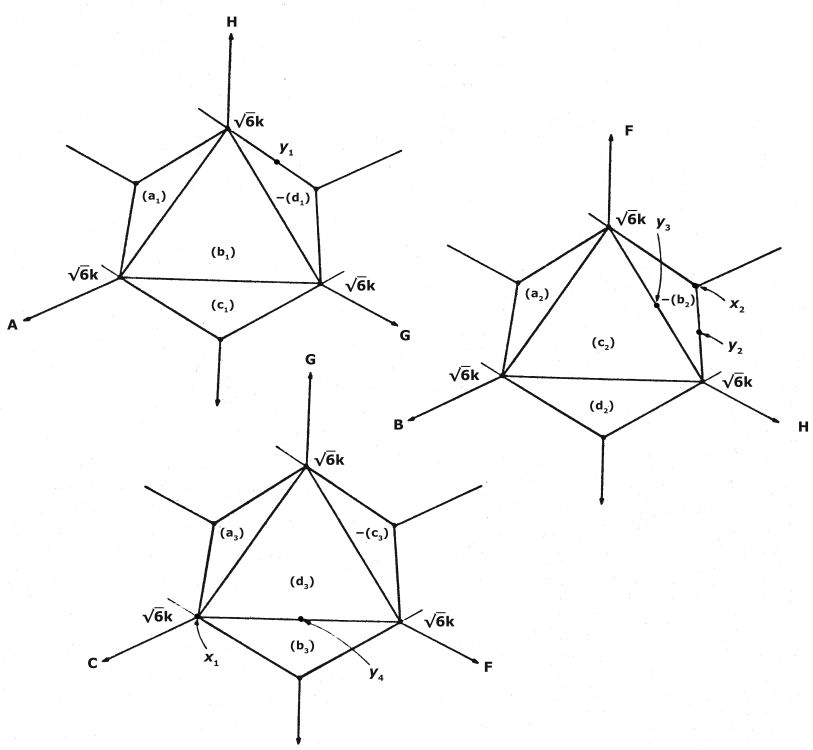

Fig. 4 Generalized Schmid's law plotted as octahedra using three separate coordinate systems

Table 3 Bishop-Hill stress states that simultaneously operate six or eight slip systems

	Stress terms					
Stress state number	A/√6 k	B/√6 k	C/√6 k	F/√6 k	G/√6 k	H/√6 k
1	1	−1	0	0	0	0
2	0	1	−1	0	0	0
3	−1	0	1	0	0	0
4	0	0	0	1	0	0
5	0	0	0	0	1	0
6	0	0	0	0	0	1
7	½	−1	½	0	½	0
8	½	−1	½	0	−½	0
9	−1	½	½	½	0	0
10	−1	½	½	−½	0	0
11	½	½	−1	0	0	½
12	½	½	−1	0	0	−½
13	½	0	−½	½	0	½
14	½	0	−½	−½	0	½
15	½	0	−½	½	0	−½
16	½	0	−½	−½	0	−½
17	0	−½	½	0	½	½
18	0	−½	½	0	−½	½
19	0	−½	½	0	½	−½
20	0	−½	½	0	−½	−½
21	−½	½	0	½	½	0
22	−½	½	0	−½	½	0
23	−½	½	0	½	−½	0
24	−½	½	0	−½	−½	0
25	0	0	0	½	½	−½
26	0	0	0	½	−½	½
27	0	0	0	−½	½	½
28	0	0	0	½	½	½

written in terms of the imposed macroscopic strain state $d\varepsilon_{k'l'}$ and substituted into Eq 6(b). The values of the 28 (56) permissible stress states contained in Table 2 are then substituted sequentially into Eq 6(b). That particular permissible stress state that maximizes dW for the given imposed strain state will operate the six or eight fcc slip systems that can accommodate this imposed strain.

Like Taylor before them, Bishop and Hill used an isostrain assumption to calculate the yield stress of an isotropic fcc crystalline aggregate in terms of the critical resolved shear stress k. Since, as shown by Bishop and Hill, their maximum work and Taylor's minimum shear criteria are equivalent, not surprisingly their value for the uniaxial yield stress of an isotropic fcc crystalline aggregate was also 3.06k.

Bounds for Yield Loci from Two-Dimensional Sachs and Bishop-Hill Averages

The isostress and isostrain approaches to calculating the uniaxial yield stress of an isotropic fcc aggregate in terms of the critical resolved shear stress k can be generalized to two dimensions to calculate yield loci for single crystals or ideal textural components (Ref 9). Individual single-crystal yield loci can then be averaged to calculate yield loci for crystalline aggregates. These rather simple two-dimensional bounds are often sufficient to answer engineering questions regarding texture hardening, for example. The basic approach is again illustrated for fcc metals deforming by rate-insensitive {111}<110> slip, but this general approach is applicable to other crystal structures with other slip behaviors as well.

Isostress or lower-bound yield loci for sheets having single-crystal orientation are found by:

- Applying a biaxial principal stress state along the rolling and transverse directions of a single-crystal or ideal texture component
- Calculating the resolved shear stresses on the 12 {111}<110> slip systems resulting from this biaxial principal stress state applied along the rolling and transverse directions
- Setting the 12 resolved shear stresses equal to k, the critical resolved shear stress
- Plotting the 12 lines representing yielding in the biaxial principal stress space
- Forming the lower-bound isostress yield locus from the intersection of these 12 lines

In general, if the rolling, transverse, and sheet normal direction are designated as r, t, and p, the six independent macroscopic stress components are σ_{rr}, σ_{tt},, σ_{pp}, σ_{rt}, σ_{tp}, and σ_{pr}. The stresses τ_{ns} acting on the {111}<110> slip systems can then be written in terms of these macroscopic stresses using the transformation:

$$\tau_{ns} = l_{nr}l_{sr}\sigma_{rr} + l_{nt}l_{st}\sigma_{tt} + l_{np}l_{sp}\sigma_{pp} + 2l_{nr}l_{st}\sigma_{rt} + 2l_{nt}l_{sp}\sigma_{tp} + 2l_{np}l_{sr}\sigma_{pr} \quad \text{(Eq 7)}$$

For example, for the ideal cube-on-corner texture, t is taken along $[1\bar{1}0]$, r is along $[11\bar{2}]$, and p is along [111]; the corresponding unit vectors are:

$$\hat{\mathbf{t}} = \frac{1}{\sqrt{2}}(\hat{\mathbf{i}}_1 - \hat{\mathbf{i}}_2), \hat{\mathbf{r}} = \frac{1}{\sqrt{6}}(\hat{\mathbf{i}}_1 + \hat{\mathbf{i}}_2 - 2\hat{\mathbf{i}}_3), \quad \text{and}$$
$$\hat{\mathbf{p}} = \frac{1}{\sqrt{3}}(\hat{\mathbf{i}}_1 + \hat{\mathbf{i}}_2 + \hat{\mathbf{i}}_3)$$

Calculating the direction cosines using the appropriate dot products and substitution into Eq 7 give the expressions in Table 4.

A lower bound to the yield locus for this ideal cube-on-corner crystal can be found directly from the equations in Table 4 by setting $\sigma_{pp} = \sigma_{rt} = \sigma_{tp} = \sigma_{tr} = 0$. The operation of each slip system will be governed by a line in σ_{rr}–σ_{tt} space; the intersections of these lines form the lower bound to the yield locus for the ideal cube-on-corner crystal (Fig. 5).

A similar procedure is used to relate the strain increments along the rolling, transverse, and sheet normal directions of the ideal cube-on-corner orientation and the summed contributions from the 12 crystallographic shears, yielding:

$$d\varepsilon_{rr} = \frac{1}{3\sqrt{6}}(-2b_1 + 2b_2 - 3c_1 + c_2 + 2c_3 - d_1 + 3d_2 - 2d_3)$$

$$d\varepsilon_{tt} = \frac{1}{\sqrt{6}}(c_1 - c_2 + d_1 - d_2)$$

$$d\varepsilon_{pp} = \frac{2}{3\sqrt{6}}(b_1 - b_2 + c_2 - c_3 - d_1 + d_3)$$

$$d\varepsilon_{rt} = \frac{1}{3\sqrt{2}}(-b_1 - b_2 + 2b_3 - c_1 + c_3 - d_2 + d_3)$$

$$d\varepsilon_{tp} = 1/12(-3a_1 - 3a_2 + 6a_3 - b_1 - b_2 + 2b_3 - c_1 - 3c_2 + 4c_3 - 3d_1 - d_2 + 4d_3)$$

$$d\varepsilon_{pr} = \frac{1}{12\sqrt{3}}(9a_1 - 9a_2 + 7b_1 - 7b_2 + 3c_1 - 5c_2 + 2c_3 + 5d_1 - 3d_2 - 2d_3)$$

(Eq 8)

These strain-slip equations are used subsequently.

An upper bound to the yield locus for this same crystal is be found by:

- Imposing different ratios of the principal strains ε_{rr} and ε_{tt}
- Transforming these principal strains to the cubic axes
- Using the maximum work principle to select the Bishop-Hill stress state that operates the slip systems necessary to accommodate this strain imposed along the cubic axes
- Transforming these Bishop-Hill stresses to the rolling (r), transverse (t), and sheet normal (p) coordinate system and supplementing these stresses with the condition that $\sigma_{pp} = 0$
- Plotting the results in σ_{rr}–s_{tt} space

Table 4 Stress transformation in Bishop-Hill notation

Slip system	Shear stress expression
$\pm(a_1)$	$-\frac{1}{2}\sigma_{tp} + \frac{1}{2}\sqrt{3}\sigma_{pr} = \pm\sqrt{6}$ k
$\pm(a_2)$	$-\frac{1}{2}\sigma_{tp} - \frac{1}{2}\sqrt{3}\sigma_{pr} = \pm\sqrt{6}$ k
$\pm(a_3)$	$\sigma_{tp} = \pm\sqrt{6}$ k
$\pm(b_1)$	$-\frac{2}{3\sqrt{6}}\sigma_{rr} + \frac{2}{3\sqrt{6}}\sigma_{pp} - \frac{2}{3\sqrt{2}}\sigma_{rt} - \frac{1}{6}\sigma_{tp} + \frac{7}{6\sqrt{3}}\sigma_{pr} = \pm\sqrt{6}$ k
$\pm(b_2)$	$\frac{2}{3\sqrt{6}}\sigma_{rr} - \frac{2}{3\sqrt{6}}\sigma_{pp} - \frac{2}{3\sqrt{2}}\sigma_{rt} - \frac{1}{6}\sigma_{tp} - \frac{7}{6\sqrt{3}}\sigma_{pr} = \pm\sqrt{6}$ k
$\pm(b_3)$	$\frac{4}{3\sqrt{2}}\sigma_{rt} + \frac{1}{3}\sigma_{tp} = \pm\sqrt{6}$ k
$\pm(c_1)$	$-\frac{1}{\sqrt{6}}\sigma_{rr} + \frac{1}{\sqrt{6}}\sigma_{tt} - \frac{2}{3\sqrt{2}}\sigma_{rt} - \frac{1}{6}\sigma_{tp} + \frac{1}{2\sqrt{3}}\sigma_{pr} = \pm\sqrt{6}$ k
$\pm(c_2)$	$\frac{1}{3\sqrt{6}}\sigma_{rr} - \frac{1}{\sqrt{6}}\sigma_{tt} + \frac{2}{3\sqrt{6}}\sigma_{pp} - \frac{1}{2}\sigma_{tp} - \frac{5}{6\sqrt{3}}\sigma_{pr} = \pm\sqrt{6}$ k
$\pm(c_3)$	$\frac{2}{3\sqrt{6}}\sigma_{rr} - \frac{2}{3\sqrt{6}}\sigma_{tt} + \frac{2}{3\sqrt{2}}\sigma_{rt} + \frac{2}{3}\sigma_{tp} + \frac{1}{3\sqrt{3}}\sigma_{pr} = \pm\sqrt{6}$ k
$\pm(d_1)$	$-\frac{1}{3\sqrt{6}}\sigma_{rr} + \frac{1}{\sqrt{6}}\sigma_{tt} - \frac{2}{3\sqrt{6}}\sigma_{pp} - \frac{1}{2}\sigma_{tp} + \frac{5}{6\sqrt{3}}\sigma_{pr} = \pm\sqrt{6}$ k
$\pm(d_2)$	$\frac{1}{\sqrt{6}}\sigma_{rr} - \frac{1}{\sqrt{6}}\sigma_{tt} - \frac{2}{3\sqrt{2}}\sigma_{rt} - \frac{1}{6}\sigma_{tp} - \frac{1}{2\sqrt{3}}\sigma_{pr} = \pm\sqrt{6}$ k
$\pm(d_3)$	$-\frac{2}{3\sqrt{6}}\sigma_{rr} + \frac{2}{3\sqrt{6}}\sigma_{pp} + \frac{2}{3\sqrt{2}}\sigma_{rt} + \frac{2}{3}\sigma_{tp} - \frac{1}{3\sqrt{3}}\sigma_{pr} = \pm\sqrt{6}$ k

Using the maximum work principle, the resulting Bishop-Hill stress states for this crystal to accommodate biaxial principal strains in the ideal cube-on-corner crystal are No. 6, 24, 25, and 28, the specific stress state depending on the imposed strain ratio. After performing the transformation outlined previously, there results the upper-bound yield locus shown in Fig. 6.

Figures 5 and 6, together with the normality condition (Ref 4, 5), are used to determine bounds for the biaxial stresses needed to enforce a specific strain state (in this case plane strain) as well as to illustrate the physical differences between these two bounds for the plane-strain yield stress.

Applying the normality condition as shown in Fig. 5, plane strain in the transverse direction ($d\varepsilon$ horizontal), one sees that the biaxial stress state needed to initiate this deformation is:

$$\sigma_{rr} = \sigma_{tt} = \tfrac{3}{2}\sqrt{6}k$$

This stress state simultaneously operates two branches of the yield locus; the first (horizontal) branch of the yield locus initiates yielding on systems $-(b_1)$, $+(b_2)$, $+(c_3)$, and $-(d_3)$; the second on systems $-(c_2)$ and $+(d_1)$.

Before proceeding further, it should first be noted that the strains $d\varepsilon_{rr}$ and $d\varepsilon_{tt}$ that result from the operation of each particular system are normal to their respective branch of the yield locus. Focusing first on the horizontal branch and letting slip occur by a unit amount in any one of the systems $-(b_1)$, $+(b_2)$, $+(c_3)$, and $-(d_3)$, the strain state from Eq 8 for each of these four systems is:

$$d\varepsilon_{rr} = -d\varepsilon_{pp} = \frac{2}{3\sqrt{6}}d\varepsilon \text{ and } d\varepsilon_{tt} = 0$$

which is normal to the horizontal branch. Similarly, if slip occurs by a unit amount on either system $-(c_2)$ or (d_1), the resulting strain is:

$$d\varepsilon_{rr} = -\frac{\sqrt{6}}{3}, d\varepsilon_{tt} = \sqrt{6}, \quad \text{and} \quad d\varepsilon_{pp} = -\frac{2\sqrt{6}}{3}$$

which again is perpendicular to its branch of the yield locus. This two-dimensional normality holds true even if the biaxial principal stresses activate systems that result in shear strains as well as normal strains; that is, the principal directions of stress and strain do not coincide.

Plane strain in the transverse direction of the cube-on-corner crystal is achieved by combining the strain vectors normal to the two branches of the yield locus to achieve the strain state $d\varepsilon_{rr} = 0$, $d\varepsilon_{tt} = 1$, and $d\varepsilon_{pp} = -1$. This is achieved by adjusting the amounts of shear on the operative systems to be:

$$b_1 = d_3 = -\frac{\sqrt{6}}{8}, b_2 = c_3 = \frac{\sqrt{6}}{8}, c_2 = -\frac{\sqrt{6}}{2}, \text{ and}$$
$$d_1 = \frac{\sqrt{6}}{2}$$

Substituting these values into Eq 8 results in plane strain in the transverse direction, since $d\varepsilon_{rr} = 0$, $d\varepsilon_{tt} = 1$, and $d\varepsilon_{pp} = -1$. However, only two of the shear strains, $d\varepsilon_{rt}$ and $d\varepsilon_{tp}$, vanish; the remaining shear strain ($d\varepsilon_{pr}$) is equal to:

$$\frac{15\sqrt{2}}{8}$$

In order to impose a state of transverse plane strain in the absence of shear strain on this cube-on-corner crystal, it is necessary both to alter the levels of σ_{rr} and σ_{tt} and to apply an additional shear stress σ_{pr}. After transforming Bishop-Hill stress state No. 6:

$$\sigma_{12} = \sqrt{6}k$$

to the r, t, and p coordinate system and imposing the condition that $\sigma_{pp} = 0$, one finds that:

$$\sigma_{rr} = \frac{\sqrt{6}}{3}k, \sigma_{tt} = \frac{5\sqrt{6}}{3}k, \sigma_{pr} = -\frac{2\sqrt{3}}{3}k, \text{ and}$$
$$\sigma_{pp} = \sigma_{rt} = \sigma_{tp} = 0$$

By substituting these stresses into Eq 8, one can verify that the critical resolved shear stress is

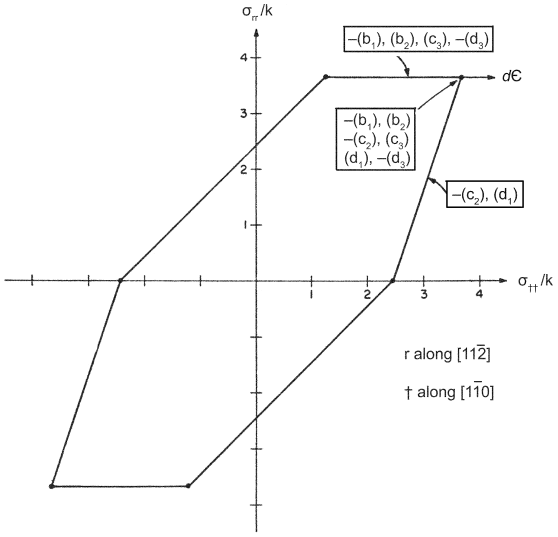

Fig. 5 Lower-bound yield locus for ideal cube-on-corner texture. Sheet normal is [111].

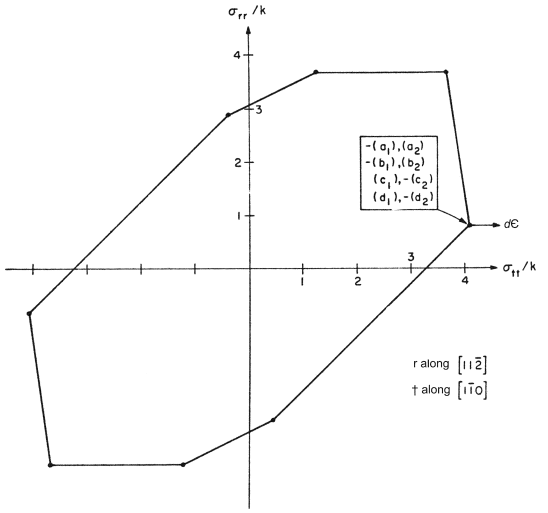

Fig. 6 Upper-bound yield locus for ideal cube-on-corner texture. Sheet normal is [111].

reached simultaneously on systems $-(a_1)$, (a_2), $-(b_1)$, (b_2), (c_1), $-(c_2)$, (d_1), and $-(d_2)$. Plane strain in the absence of shear strain can be achieved if the amounts of shear on these operative systems are:

$$a_1 = \frac{\sqrt{6}}{6}, a_2 = -\frac{\sqrt{6}}{6}, b_1 = -\frac{\sqrt{6}}{2}, b_2 = \frac{\sqrt{6}}{2}, c_1 = d_1 = \frac{\sqrt{6}}{4}, \text{ and } c_2 = d_2 = -\frac{\sqrt{6}}{4}$$

Thus, for the ideal cube-on-corner orientation, transverse plane strain in the absence of shear stress is accompanied by the additional shear strain $d\varepsilon_{pr}$; transverse plane strain in the absence of shear strain, on the other hand, requires the additional shear stress σ_{pr}. Hence, in neither case do the principal directions of stress and strain coincide. This lack of coincidence of the principal directions is not restricted to the cube-on-corner orientation. It should also be pointed out that the aforementioned solution for the amounts of shear needed to accommodate transverse plane strain in this ideal cube-on-corner orientation is not unique. Hence, the accompanying rotations leading to textural changes are not unique as well.

There are various ways in which the slip behaviors of multiple-crystal orientations can be combined to find yield loci for crystalline aggregates. One such average is the original yield locus for an isotropic fcc polycrystalline aggregate calculated by Bishop and Hill (Ref 5). Their averaging process rounded the edges that resulted from the intersections of the lines governing the operation of specific slip systems and resulted in a yield locus that is midway between the Tresca and the von Mises locus. Since the Bishop-Hill procedure is based on an isostrain model (violating stress continuity among grains), this yield locus is an upper bound to the actual locus.

Recent Developments

The lack of a unique prediction of operative slip systems resulting from the rate-insensitive Bishop-Hill procedure was remedied by using a rate-sensitive model, first introduced by Hutchinson (Ref 10). An example of a computer code that incorporates rate sensitivity is the widely used Los Alamos polycrystal plasticity (LApp) code (Ref 11, 12). The LApp is a modified Taylor isostrain model that incorporates not only rate sensitivity but also grain shape and relaxed constraints (Ref 12).

Several slip behaviors other than <111>{110} slip in fcc metals have been studied in some detail. It should again be pointed out that <111>{110} slip in fcc metals is equivalent to <110>{111} slip in body-centered cubic (bcc) metals (often referred to as restricted glide), since this only involves switching the identities of the angles λ and ϕ and hence leaves Schmid's law unchanged. Another approach to modeling bcc slip behavior is pencil glide, where slip is assumed to occur with equal ease on the most highly stressed planes containing the <111> slip directions (Ref 13). This slip plane relaxation has resulted in a change of the Taylor factor for an isotropic crystalline aggregate from 3.06 for bcc restricted glide to 2.73 for bcc pencil glide (Ref 14). The plastic deformation of hexagonal close-packed (hcp) crystals has also been studied (Ref 15, 16). Modeling the plastic behavior of hcp metals is inherently more complicated, because deformation typically occurs by twinning in addition to slip (Ref 12).

While most current computer modeling efforts are isostrain based (Taylor or Bishop and Hill), many problems, especially those associated with surface behavior, are better described using simpler crystallographic approaches. A case in point is the characterization of surface roughening during plane-strain plastic deformation of aluminum alloy sheet (Ref 17). Orientation imaging and scanning electron microscopy of individual surface grains were used to characterize surface roughening resulting from the presence of both slip-banded valley-forming grains and nonslip-banded hill-forming grains. What was found was that slip-banded valley-forming grains correlated with Schmid factor-based unconstrained measures rather than constrained measures based on the Taylor factor. This is but one example of the caution needed to select the plasticity model appropriate to the problem being addressed.

REFERENCES

1. E. Schmid, *Proc. Intern. Congr. Appl. Mech., Delft, 1924*, p 342–352, J. Waitman, Jr., Delft, 1925
2. G. Sachs, Zur Ableitung einer Fliessbedingung, *Z. Ver. deut.Eng.*, Vol 72, p 734–736, 1928
3. W.A. Backofen, W.F. Hosford, Jr., and J.J. Burke, Texture Hardening, *Trans. ASM*, Vol 55, p 264, 1962

4. J.F.W. Bishop and R. Hill, A Theory of the Plastic Distortion of a Polycrystalline Aggregate under Combined Stresses, *Phil. Mag*., Vol 42, p 414, 1951
5. J.F.W. Bishop and R. Hill, A Theoretical Derivation of the Plastic Properties of a Polycrystalline Face-Centered Metal, *Phil. Mag*., Vol 42, p 1298, 1951
6. J.F.W. Bishop, A Theoretical Examination of the Plastic Deformation of Crystals by Glide, *Phil. Mag*., Vol 44, p 51, 1953
7. R. von Mises, Mechanik der plastischen Formanderung der Kristallen, *Z. Angew. Math. Mech*., Vol 8, p 161, 1928
8. G.I. Taylor, Plastic Strain in Metals, *J. Inst. Metals*, Vol 62, p 307, 1938
9. H.R. Piehler and W.A. Backofen, The Prediction of Anisotropic Yield Loci for Textured Sheets, *Textures in Research and Practice*, G. Wassermann and G. Grewen, Ed., Springer Verlag, Berlin, 1969, p 436–443
10. J.W. Hutchinson, Bounds and Self-Consistent Estimates for Creep of Polycrystalline Materials, *Proc. Roy. Soc. London A,* Vol 348, No. 1652, (Feb. 10, 1976), p 101–127
11. U.F. Kocks, G.R.Canova, C.N. Tome, A.D. Rollett, and S.I. Wright, *Computer Code LA-CC-88-6* (Los Alamos, NM: Los Alamos National Laboratory)
12. U.F. Kocks, C.N. Tome, and H.-R. Wenk, *Texture and Anisotropy*, Cambridge University Press, 1998
13. H.R. Piehler and W.A. Backofen, A Theoretical Examination of the Plastic Properties of Body-Centered Cubic Crystals Deforming by <111> Pencil Glide, *Met. Trans.,* Vol 2, p 249–255, 1971
14. J.M. Rosenberg and H.R. Piehler, Calculation of the Taylor Factor and Lattice Rotations for Bcc Metals Deforming by Pencil Glide, *Met. Trans*., Vol 2, p 257–259, 1971
15. D.R. Thornburg and H.R. Piehler, An Analysis of Constrained Deformation by Slip and Twinning in Hexagonal Close-Packed Metals and Alloys, *Met. Trans. A*, Vol 6A, p 1511–1523, 1975
16. C. Tome and U.F. Kocks, The Yield Surface of HCP Single Crystals, *Acta Metall*, Vol 33, p 603–621, 1985
17. Y.S. Choi, H.R. Piehler, and A.D. Rollett, Formation of Mesoscale Roughening in 6022-T4 Al Sheets Deformed in Plane-Strain Tension, *Met. and Mat. Trans. A*, Vol 35A, p 513–524, 2004